



# Elastic properties of quaternary glasses in the MgO–CaO–Al<sub>2</sub>O<sub>3</sub>–SiO<sub>2</sub> system: modelling versus measurement

Ulrike Veit<sup>1,\*</sup>  and Christian Rüssel<sup>1</sup>

<sup>1</sup> Otto-Schott-Institut, Jena University, Fraunhoferstr. 6, 07743 Jena, Germany

**Received:** 22 December 2016

**Accepted:** 16 March 2017

**Published online:**  
23 March 2017

© Springer Science+Business  
Media New York 2017

## ABSTRACT

The elastic properties of quaternary glass-forming systems within the CaO–MgO–Al<sub>2</sub>O<sub>3</sub>–SiO<sub>2</sub> composition were evaluated. Their compositions differed by not more than 3 mol% for each component from each other. After melting, the exact chemical compositions were determined using X-ray fluorescence, and the densities were measured by Archimedes method and pycnometer. This property and its dependency upon small variations in the composition are the main focuses of this paper. Experimental elastic properties such as Poisson's ratio and Young's modulus were calculated by measured ultrasound wave velocities (longitudinal and shear) at room temperature. Model calculations of the Poisson's ratios were not in satisfying agreement with the measured results. The experimentally determined data of the Young's modulus values ranging between 87 and 91 GPa were compared to different model calculations, which were mostly smaller than the measured ones, ranging—depending on the model—between 70 and 93 GPa. The effect of MgO was also studied by comparing the glasses with similar compositions without any MgO.

## Introduction

The ternary systems CaO–Al<sub>2</sub>O<sub>3</sub>–SiO<sub>2</sub> and MgO–Al<sub>2</sub>O<sub>3</sub>–SiO<sub>2</sub> with minor additions of different network modifiers have been studied extensively with respect to their crystallization behaviour for possible use in hard disc substrates [1] or in dentistry [2, 3]. Furthermore, the glass systems are commonly used for fibre glass production in order to meet requirements for numerous applications [4–6], and they were proposed as laser materials as well [7–9]. The

quaternary glass-forming system CaO–MgO–Al<sub>2</sub>O<sub>3</sub>–SiO<sub>2</sub> (CMAS) is of particular interest, because of its inexpensive raw materials, its high corrosion resistance and its good mechanical properties. This is why these compositions have received much attention in scientific research [2, 3, 6, 10–15].

Glasses are known to be brittle, if exposed to mechanical or thermal stresses—unlike plastic and metals. The knowledge on mechanical properties and hence the mechanical strength is a crucial factor for structural applications of materials and is required

Address correspondence to E-mail: Ulrike.Veit@uni-jena.de

for the right choice of the most appropriate material for a particular application. Although all the characters of applied force, temperature, shape and surface defects significantly affect the strength of a glass product, the elastic properties are usually directly related to the Young's modulus [16]. According to Griffith's theory, the strength of materials increases with their elastic moduli but is also crucially dependent on the number and geometry of the defects, especially of micro-cracks [16].

An extensive number of publications on the structural and acoustic properties of multicomponent silicate glasses can be found in the literature [8, 17–22]. One of the best available techniques to investigate the acoustic properties of materials is the ultrasonic non-destructive pulse-echo technique because of the close association of the ultrasonic waves with the elastic and the inelastic properties of the materials [20].

The mechanical properties are highly dependent on the composition and upon the structure as well; the acoustic properties are also connected with those parameters. If multicomponent oxide glasses are assumed as solution of oxides in which each oxide has its own effect and no definite combinations occur, any structural or physical glass property as a whole can logically be considered as the sum of the effects of all individual oxides [19].

To overcome the problems of the classical time-consuming experimental procedure, coupling of modelling (optimization) and experiments is the means of choice. The key experimental conditions can be identified based on the pre-existing modelling results; afterwards experimental results can be used for the improvement in modelling. Hence, time and costs to perform experiments can be significantly decreased. The calculation of the Young's modulus ( $E$ ) from the glass composition is advantageous for the development of glassy materials. Hence, many authors worked on models for the empirical calculation to enable an a priori assessment of Young's modulus [17, 18, 23–26].

To improve the long-term strength and longevity of materials and also properties such as corrosion resistance, it is needed to substitute alkali oxides by modifier oxides of higher valency. In this context, alkaline earth oxides such as CaO and MgO are of special interest. It was shown that magnesium oxide and calcium oxide as network modifiers affect the structure of the glass network [27]. The induced change in density could possibly affect the Young's

modulus as well. It has been shown that MgO increases the strength of aluminosilicate glass ceramics [28]. But the influence of magnesium ions on the elastic properties of glasses is not yet clearly described, especially if also other network modifiers occur.

For this work, glass compositions in the quaternary system CaO–MgO–Al<sub>2</sub>O<sub>3</sub>–SiO<sub>2</sub> (CMAS) without the addition of alkali oxides were prepared. Twenty-eight glasses within this system were melted and characterized. The chemical composition determined by X-ray fluorescence (XRF), the density (for more information, see Ref. [27]) and the acoustic properties were evaluated for each glass composition. The measured XRF data were used for further correlations of physical properties and to minimize the error if simulated and measured results were compared. The values of Young's modulus derived from experimental data were compared with different empirical models proposed by Makishima–Mackenzie [17, 18], Rocherulle et al. [23] and Priven [24]. Also, the ultrasound velocities were computed using empirical models. A correlation between the structure and the elastic properties of these glasses was also discussed. Furthermore, Young's moduli were compared with those of some glasses which did not contain MgO (from Ref. [15]).

## Experimental procedure

Table 1 shows the chemical compositions of all studied 28 glasses. The used raw materials were pure quartz of grain size C, CaCO<sub>3</sub> and Al(OH)<sub>3</sub> and 4MgCO<sub>3</sub> × Mg(OH)<sub>2</sub> × 5H<sub>2</sub>O (all Merck AG).

The concentration of each component does not differ by more than 3 mol% from that of the base glass composition 61.2 SiO<sub>2</sub>, 26.3 mol% CaO, 8.6 mol% Al<sub>2</sub>O<sub>3</sub> and 3.8 mol% MgO. This composition range was studied because the liquidus temperatures  $T_{\text{Liq}}$  are lower than 1300 °C and hence comparatively low. These compositions are advantageous because relatively low melting temperatures are necessary, and hence, an energy and environmentally advantageous production is possible [29]. Furthermore, they are fairly stable against devitrification.

The raw materials for 350 g glass were mixed by manual shaking. A portion of the powder mixture was filled into a platinum crucible, which was

**Table 1** XRF values and nominal composition of glasses in mol%, calculated effective molar mass  $M_{\text{eff}}$ , calculated molar volume  $V_M$  and the calculated number of bridging oxygen per tetrahedron BO/T

Glass	Nominal compositions				XRF results normalized				$M_{\text{eff}}$ (g/mol)	$V_M$ (cm <sup>3</sup> /mol)	BO/T
	SiO <sub>2</sub> (mol%)	CaO (mol%)	Al <sub>2</sub> O <sub>3</sub> (mol%)	MgO (mol%)	SiO <sub>2</sub> (mol%)	CaO (mol%)	Al <sub>2</sub> O <sub>3</sub> (mol%)	MgO (mol%)			
1	60.54	27.44	8.75	3.27	60.88	26.98	8.90	3.23	62.09	23.20	3.46
2	62.25	25.33	9.14	3.28	62.58	24.75	9.27	3.41	62.30	23.53	3.53
3	61.22	26.30	8.64	3.84	61.66	25.68	8.79	3.87	61.97	23.25	3.48
4	61.24	25.23	9.10	4.42	61.60	24.51	9.23	4.67	62.04	23.35	3.50
5	59.81	25.62	9.56	5.01	60.18	24.86	9.59	5.38	62.04	23.23	3.48
6	60.12	27.25	8.24	4.39	60.17	26.73	8.27	4.83	61.52	22.92	3.39
7	59.86	28.58	8.86	2.70	60.61	27.87	9.00	2.52	62.24	23.21	3.46
8	62.52	27.12	7.68	2.68	63.11	26.38	7.82	2.70	61.76	23.27	3.46
9	59.30	28.14	7.62	4.93	59.86	27.34	7.78	5.03	61.27	22.73	3.35
10	61.67	25.8	8.13	4.39	62.36	25.19	8.28	4.18	61.71	23.24	3.47
11	61.87	26.71	8.16	3.26	62.75	25.75	8.32	3.18	61.90	23.31	3.48
12	60.52	25.96	9.10	4.42	60.66	25.51	9.23	4.60	62.01	23.26	3.47
13	61.25	27.33	8.16	3.26	61.68	26.57	8.28	3.47	61.80	23.21	3.44
14	62.31	25.32	9.09	3.28	63.02	24.66	9.23	3.09	62.35	23.57	3.55
15	61.88	25.14	8.57	4.41	61.82	24.38	8.62	5.18	61.69	23.12	3.47
16	61.29	28.36	7.68	2.68	61.83	27.89	7.81	2.48	61.74	22.87	3.42
17	63.42	24.32	9.54	2.72	63.56	23.72	9.60	3.12	62.53	23.71	3.58
18	59.03	28.19	7.84	4.94	58.61	27.42	7.87	6.10	61.07	22.63	3.31
19	60.26	27.23	8.13	4.39	59.82	27.54	8.00	4.65	61.41	22.77	3.36
20	62.12	25.30	7.63	4.94	63.04	24.75	7.80	4.41	61.48	23.22	3.46
21	61.27	24.15	9.57	5.01	62.52	23.80	9.72	3.96	62.42	23.58	3.56
22	63.30	24.34	9.64	2.72	64.57	23.55	9.77	2.11	62.81	24.00	3.62
23	60.71	26.88	9.13	3.28	60.91	25.89	9.19	4.01	62.10	23.33	3.48
24	62.54	23.99	8.50	4.98	63.00	23.59	8.72	4.70	61.86	23.26	3.51
25	60.21	27.46	9.62	2.71	60.28	26.36	9.73	3.62	62.39	23.38	3.49
26	59.30	28.14	7.62	4.93	59.94	27.18	7.81	5.07	61.26	22.73	3.35
27	61.88	25.14	8.57	4.41	62.58	24.23	8.75	4.44	61.90	23.28	3.50
28	61.27	26.26	8.62	3.846	61.44	25.75	8.69	4.12	61.87	23.21	3.46

transferred to a Super-Kanthal furnace (MoSi<sub>2</sub> heating elements) and then heated up until the main part of carbon dioxide was evaporated and the batch had been fully sintered. Then, the next part of the raw materials was added. Subsequently, the temperature was increased to 1590 °C and held for two h or more for fining.

In order to achieve fast cooling, the melt was cast in 10 l of cold water and then dried at 120 °C. This procedure was supplied to increase the homogeneity of the glass. Subsequently, the glass was remelted at 1600 °C, kept for 3 h at this temperature and finally cast. For this purpose, two heat resistant steel (AL7) moulds were coated with boron nitride by using a spray and then preheated to 600 °C. The crucible

with the residual, adherent glass was then transferred again to the melting furnace and, after reheating, cast into the second mould. For thermal annealing, the glass was transferred to a cooling furnace preheated to temperatures slightly above the glass transition temperature,  $T_g$ , that is in the range from 775 to 805 °C depending on the glass composition. All glasses were cooled using the same procedure, and hence, a direct comparison of the densities and glass transition temperatures  $T_g$  is enabled although these properties might have only a slight effect on the cooling history [30]. The second glass block of each glass showed some striae. For the characterization of the density, only the first block was used.

The chemical composition of the glasses was determined by X-ray fluorescence (XRF) using a PANalytical MagixPro (4 kW Rh Tube).

The densities of the glasses were measured using a helium pycnometer (AccuPyc 1330, Micromeritics GmbH, Germany). The maximum size of the glass samples in the Accupyc 1330 is  $15 \times 15 \times 30 \text{ mm}^3$ . Furthermore, the density values were compared to values determined using the Archimedes method (buoyancy method) according to ASTM Standard C693-93 [31]. For this purpose, a high precision scale MC1 Analytik AC210 P (Fa. Sartorius AG, Göttingen) with a specific density accessory was used.

Young's moduli were measured using the ultrasound technique by Krautkrämer (USD 15 Krautkrämer-Branson, Austria) at room temperature [32]. The used glass samples were 20- to 30-mm-long cylinders with a diameter of 15 mm, the same as that of the transducer ( $\varnothing 15 \text{ mm}$ ). Both edges were parallel to each other with deviations of less than 0.5 mm. By using this method, the longitudinal and transversal acoustic velocities were determined. The ultrasonic wave velocities were measured by using a pulse-echo technique, whereas the frequency of the longitudinal and transversal probes was 5 and 4 MHz, respectively. In particular, the elapsed time between the initiation and the receipt of the pulse was determined. The velocity  $v$  was then calculated by dividing the roundtrip distance  $2a$  by the elapsed time  $\Delta t$  (see Eq. 1):

$$v = \frac{2a}{\Delta t} \quad (1)$$

where  $a$  is the thickness of the sample and  $\Delta t$  is the time interval from the initiation to the receipt of the pulse. The space between transducer and sample was filled with honey, which serves to couple the shear waves. From the respective velocities, the Poisson's ratio  $\nu$  is calculated by Eq. 2:

$$\nu = \frac{\frac{1}{2} - \left(\frac{v_t}{v_l}\right)^2}{1 - \left(\frac{v_t}{v_l}\right)^2} \quad (2)$$

where  $v_t$  and  $v_l$  are the shear (transversal) and the longitudinal sound velocities within the sample, respectively.

The Young's modulus  $E$  (in GPa) is finally calculated by Eq. 3 [33]:

$$E = 2\rho v_t^2(1 + \nu) = \frac{2\rho v_t^2}{1000000} \times \left[ 1 + \frac{0.5 - \left(\frac{v_t}{v_l}\right)^2}{1 - \left(\frac{v_t}{v_l}\right)^2} \right] \quad (3)$$

where  $\rho$  in  $\text{g/cm}^3$  is the density of the glass sample and the  $v_t$  and  $v_l$  are the phase velocities given in  $\text{m/s}$ .

The theoretical maximum error propagation  $\Delta E$  of the sonic modulus  $E$  (due to the random error of the measurement) can then be calculated as follows:

$$\Delta E = \sqrt{\left(\frac{\delta E}{\delta \rho} \times |\Delta \rho|\right)^2 + \left(\frac{\delta E}{\delta v_t} \times |\Delta v_t|\right)^2 + \left(\frac{\delta E}{\delta v_l} \times |\Delta v_l|\right)^2} \quad (4)$$

because the density  $\rho$  and the sound velocities  $v_t$  and  $v_l$  are the parameters, which show random machine errors of  $\pm 0.005 \text{ g/cm}^3$  and  $\pm 30 \text{ m/s}$ , respectively. Their errors have to be included in the error propagation calculation. Each differentiation of the parameters is given by the following equations and needs to be multiplied with its own systematic error:

$$\frac{\delta E}{\delta \rho} = \left[ 1 + \frac{0.5 - \left(\frac{v_t}{v_l}\right)^2}{1 - \left(\frac{v_t}{v_l}\right)^2} \right] \times \frac{v_t^2}{500000} \quad (5)$$

$$\frac{\delta E}{\delta v_t} = \frac{2v_l v_t^4}{250000 \times (v_t^2 - v_l^2)^2} - \frac{\rho v_t^4}{500000 \times v_l^3 \times \left(1 - \left(\frac{v_t}{v_l}\right)^2\right)^2} \quad (6)$$

$$\frac{\delta E}{\delta v_l} = \frac{\rho v_t}{250000} + \frac{\rho v_t}{500000 \times \left(1 - \left(\frac{v_t}{v_l}\right)^2\right)} + \frac{\rho v_t^3}{500000 \times v_l^2 \times \left(1 - \left(\frac{v_t}{v_l}\right)^2\right)^2} - \frac{\rho v_t^3}{125000 v_l^2 \times \left(1 - \left(\frac{v_t}{v_l}\right)^2\right)} - \frac{\rho v_t^5}{250000 v_l^4 \times \left(1 - \left(\frac{v_t}{v_l}\right)^2\right)^2} \quad (7)$$

The propagation error of the measured sample is around 1.34 GPa—depending on the results of the phase velocities and the density.

The molar volumes of the glasses are calculated by Eq. 8

$$V_M = \frac{\sum x_i M_i}{\rho} \quad (8)$$

where  $\rho$  is the glass density,  $x_i$  and  $M_i$  are the mole fraction and the molecular weight of the oxide component  $i$ , respectively.

## Results and discussion

The glass transition temperatures  $T_g$  of the glasses vary between 754 and 783 °C, which is lower than the  $T_g$  of the calcium–aluminosilicate glass system without MgO, as reported in Ref. [15]. As stated in Ref. [34], the relaxation times of glasses at  $T_g$  are only few minutes. Within that time, the residual stresses in the melted glasses are gradually eliminated with increasing annealing time. Since all glass transition temperatures are well below 850 °C, the right cooling temperature of the cooling furnace at 850 °C has been chosen and the glasses can be considered as relaxed. As reported, for example, by DeGuire [22], all properties of glasses are affected by their thermal history. The faster a glass melt is quenched, the looser is the glass network structure. Hence, the density is decreased, which in turn might affect the elastic properties as well due to a change in phase velocities in the glasses. So it is crucial to cool down and relax the glass bulk structure properly. Furthermore, no stress-induced striae were found using photoelasticity to determine the stress distribution.

It has been shown in different studies on the glass structure of alumina silicate glasses, that  $\text{Al}_2\text{O}_3$  is mostly incorporated into the glass network as  $[\text{AlO}_4]^-$ -tetrahedra. They act as a network former as long as the molar concentrations of alkali or alkali earth oxides equal or exceed those of alumina [34–36]. The charges of the  $[\text{AlO}_4]^-$ -tetrahedra need to be charge balanced by positively charged cations [35]. For metaluminous or peralkaline glasses, it is expected that all aluminium units form tetrahedra with 4/2 bridging oxygen. The mean number of bridging oxygen per network forming  $[\text{SiO}_4]^-$  and  $[\text{AlO}_4]^-$ -tetrahedra (BO/T or Q number) can be calculated from the chemical composition and is a simple measure of the connectivity and rigidity of the glasses [35, 36]. All glasses have a ratio of CaO or MgO to  $\text{Al}_2\text{O}_3$  larger than 1, which means all tested samples contain high enough concentrations of network modifiers to compensate the negative charge of

all  $[\text{AlO}_4]^-$ -tetrahedra. Hence, in all studied compositions, the  $[\text{AlO}_4]^-$ -tetrahedra are considered to be charge balanced by  $\text{Mg}^{2+}$  and  $\text{Ca}^{2+}$  ions and do not lead to a depolymerization of the network; however, any excess  $\text{Ca}^{2+}$  and  $\text{Mg}^{2+}$  ions form non-bridging oxygen (NBO) sites and hence decrease the number of Si–O–Si bridges [34]. The higher the excess of calcium or magnesium ions is, the larger is the number of non-bridging-oxygen sites and the lower is the number of bridging oxygens per tetrahedron (BO/T), and the more pronounced is the depolymerization of the glass structure. Therefore, the BO/T can be calculated by the following equation:

$$\frac{\text{BO}}{\text{T}} = 4 - \frac{2 \times (n_{\text{CaO}} + n_{\text{MgO}} - n_{\text{Al}_2\text{O}_3})}{(n_{\text{SiO}_2} + 2 * n_{\text{Al}_2\text{O}_3})} \quad (9)$$

where  $n_i$  is the concentration of the oxide in mol%.

Later on, the obtained results are also plotted against BO/T and discussed.

## XRF

In Table 1, the glass compositions determined by X-ray fluorescence (XRF) of each glass composition are compared with their target compositions. The XRF values added up to at least 99.70 mol% and were normalized to 100 mol% for better comparison.

In all samples, the calcium oxide values were 0.4 to 1.1 mol% higher than the intended CaO concentration. The rise in the CaO concentration resulted mostly in a decrease in the  $\text{SiO}_2$  and MgO concentrations, whereas  $\text{Al}_2\text{O}_3$  showed always the same shift of around 0.1 mol%. Other trace oxides were not found in the melted glass samples within the sensitivity of the used method and equipment.

The glasses 26, 27, and 28 had the same nominal compositions as the glasses 9, 15, and 3, respectively, to check the reproducibility. The glasses 9 and 26 were very similar, whereas the glass duos 27/15 and also 3/28 show shifts within the MgO and  $\text{SiO}_2$  concentrations of 0.75 and 0.22 mol%, respectively. In the following, the measured and normalized XRF data will be used for further correlations with physical properties. This also minimizes the deviation between simulated and measured densities.

## Elastic properties

The phase velocities  $v_1$  and  $v_t$  are visible in Table 2. The differences between the minimum and

**Table 2** Acoustic and mechanical properties of the glasses with two different samples from one melt with phase velocities  $c_l$  and  $c_t$ , Poisson's ratio  $\nu$ , Young's modulus  $E$

Sample	$c_l$ in m/s $\pm 30$ ms	$c_t$ in m/s $\pm 30$ ms	$\nu$ $\pm 0.006$	$K$ in GPa $\pm 5$ GPa	$G$ in GPa $\pm 0.6$ GPa	$E$ in GPa $\pm 1.3$ GPa
1	6373	3644	0.257	61.2	35.5	89.2
2	6396	3656	0.257	61.1	35.4	88.9
3	6304	3636	0.251	58.8	35.2	88.0
4	6295	3655	0.246	57.9	35.5	88.3
5	6341	3621	0.258	60.7	34.9	88.3
6	6438	3648	0.264	63.7	35.8	90.4
7	6398	3639	0.261	60.2	34.8	89.4
8	6341	3605	0.261	60.7	34.5	87.0
9	6413	3646	0.261	63.0	35.8	90.2
10	6333	3606	0.260	60.5	34.5	87.1
11	6351	3609	0.262	61.0	34.6	87.3
12	6404	3658	0.258	61.7	35.6	89.6
13	6342	3673	0.248	59.2	35.9	89.7
14	6283	3647	0.246	57.5	35.2	87.6
15	6406	3672	0.255	63.9	35.6	90.3
16	6423	3615	0.268	64.4	35.3	89.6
17	6383	3659	0.255	60.4	35.3	88.7
18	6324	3625	0.255	60.6	35.4	88.9
19	6335	3630	0.256	60.9	35.5	89.2
20	n.d.	n.d.				
21	6386	3639	0.260	61.1	35.0	88.2
22	6337	3649	0.252	58.9	35.0	87.7
23	6358	3629	0.258	60.9	35.2	88.9
24	6334	3633	0.255	59.9	35.1	88.1
25	6329	3639	0.253	59.9	35.4	88.7
26	6358	3654	0.253	60.9	36.0	90.2
27	6351	3660	0.251	59.8	35.2	89.4
28	6326	3641	0.252	59.5	35.3	88.4

maximum values for  $v_l$  and  $v_t$  are 155 and 68 m/s, respectively. Considering the maximum theoretical error margin of  $\pm 30$  m/s, these glasses do not show a large deviation in their phase velocities, especially for  $v_t$ .

It is known that a decreasing ultrasonic velocity is related to the increase in the number of non-bridging oxygen and therefore a decrease in the connectivity of the glass network, where the modifiers break the bonds of the tetrahedral  $\text{SiO}_4$  units [37].

As shown in Fig. 1, however, there is no clear correlation between the number of bridging oxygen per tetrahedral unit and the transversal and longitudinal phase velocities. The comparatively high error margin of the measurement system is probably overlying the small variations of the results for those glasses.

### Poisson's ratio

For any structure, Poisson's ratio  $\nu$  is formally defined as the ratio of lateral to longitudinal strain, produced if tensile forces are applied [38, 39]. If tensile stresses are applied parallel to the chains, the produced longitudinal strain will be the same for networks despite the linking of the network. However, the lateral strain (perpendicular to the chain) is greatest for a network with no bridging oxygen bonds (crosslink density = 0) as only ionic bonds and the weak interchain van der Waals forces contribute to the forces against contraction. The more crosslinks, i.e. the more bridging oxygen, occur within the glass network, the higher the decrease in the lateral strain. Hence, in a glass network in which the crosslink density—defined as the number of bridging oxygen

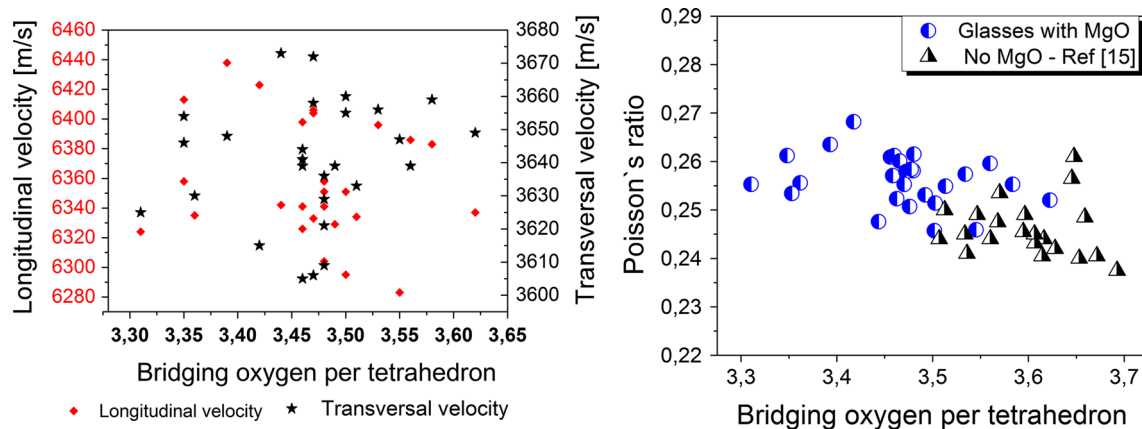


**Figure 1** Phase velocities  $v_l$  and  $v_t$  and Poisson's ratio  $\nu$  as a function of the number of bridging oxygen per tetrahedron.

per tetrahedron minus two—is doubled, the lateral strain will decrease to half of the value. Thus, the ratio of lateral to longitudinal strain,  $\nu$ , in an isotropic vitreous network with a BO/T of two (crosslink density of zero) has Poisson's ratio  $\sim 0.4$ , whereas networks with a BO/T of 3 or 4 (crosslink density of 1 or 2) lead to Poisson's ratios of  $\sim 0.3$  and  $\sim 0.15$  (f.e. pure  $\text{SiO}_2$  with BO/T = 4, crosslink density of 2), respectively [25, 38]. This is in full agreement with the results of this paper. The Poisson's ratios calculated from the ultrasonic phase velocities lie between 0.246 and 0.268, and the number of bridging oxygen of the glasses is between 3.31 and 3.62. This correlation is shown in Fig. 1, where glasses with similar compositions, however, without MgO from Ref. [15] are included. The higher the BO/T of the glass, the lower their Poisson's ratio; this means the higher the network connectivity, the lower the ratio of lateral to longitudinal strain. Even those small changes within the composition of the glasses in this study (less than 3 mol% per component) notably affect the Poisson's ratio. This has also been described by Rouxel in Ref. [38]. Hence, the Poisson's ratio shows the expected trend in dependence on the glass network structure although the phase velocities do not.

### Young's modulus

The values of Young's modulus—listed in Table 2 show only a very small (and unexpected) variation between 87 and 90.4 GPa (glass 8 and 6) even though the densities vary between  $2.631$  and  $2.700 \text{ g} \times \text{cm}^{-3}$ . The previous assumption that the addition of magnesium oxide to the different glass compositions, in varying amounts between 2 and 6 mol% MgO, would

have a greater influence on the elastic properties was proved as incorrect.

The glasses 9 and 26 with almost identical compositions have the same Young's moduli of 90.2 GPa. In analogy, the glass duo with the sample numbers 3 and 28 with similar compositions shows only small variations of 88.0 and 88.4 GPa. Within the distribution of values between 87.0 and 90.4 GPa, this is only a very small variation and is well below the possible maximum of the theoretical propagation error of  $\pm 1.34$  GPa. Hence, the determination of the elastic moduli shows a high reproducibility. Only in the case of the glasses 15 and 27, which had identical nominal compositions, more different moduli of 90.3 and 89.4 GPa were, respectively, obtained. This is easily explained by the MgO discrepancy of more than 0.7 mol% of the measured compositions of those two glasses (4.44 and 5.18 mol%).

Considering the comparatively small variation of the Young's moduli of only 3.4 GPa of the tested glasses, the maximum theoretical propagation error of the used equipment, given with  $\pm 1.34$  GPa, is a high deviation complicating the comparison and interpretation of results.

In comparison with glasses containing no magnesium oxide, the Young's moduli for the tested glasses were around 3 GPa higher. This is a significant difference, even taking the propagation error into account.

However, when interpreting Fig. 2, neither the effect of the MgO concentration nor that of the CaO concentration on the mechanical properties shows a clear trend. The Pearson correlation coefficients are 0.37 (0.43) for the correlation between MgO concentration (CaO concentration) and Young's modulus, which are comparatively small. This is due to the

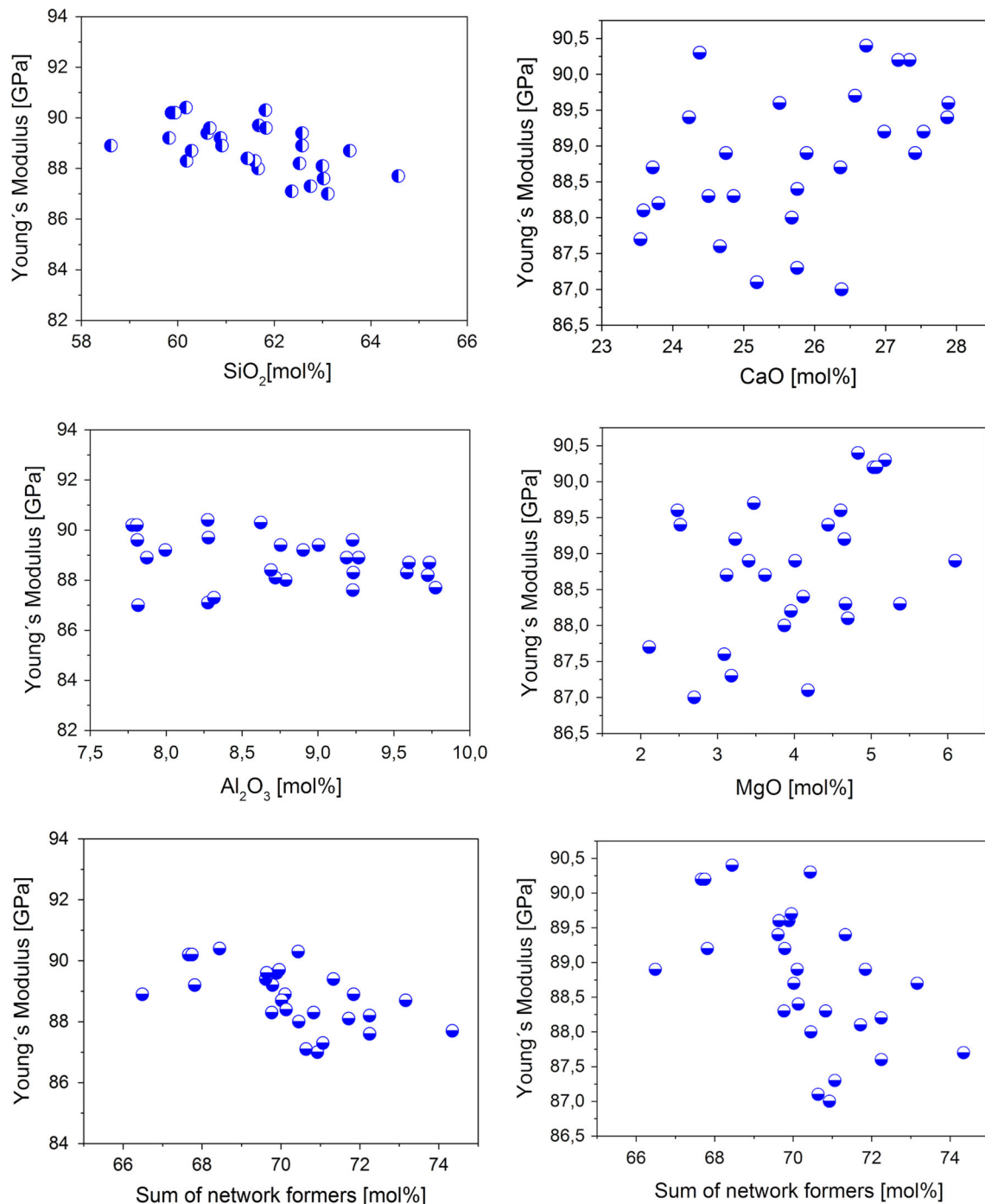


**Figure 2** Young's modulus as a function of the oxide concentration.

small variation of the Young's modulus values; thus, the error of the values is too high to enable a more detailed interpretation. The correlation coefficients for the influence of SiO<sub>2</sub> and Al<sub>2</sub>O<sub>3</sub> on the Young's modulus are  $-0.57$  and  $-0.26$ —and hence do not show a clear correlation either. The high deviation error of the experimental values is probably the

reason for this poor correlation. However, there is a visible trend to a decrease in Young's moduli with increasing concentration of network formers (negative correlation coefficients indicating an indirect proportionality). Furthermore, the positive correlation coefficients for network modifiers show a direct proportionality.



*Substitution of network formers by network modifiers*

The glasses 4 and 12 with almost identical MgO and Al<sub>2</sub>O<sub>3</sub> concentrations illustrate that the substitution of SiO<sub>2</sub> by CaO results in increasing Young's moduli just as expected. Other examples that show similar behaviour are the glass sets 16 and 8 and 11 and 13.

The substitution of SiO<sub>2</sub> by MgO leads to a similar effect. For the glass sets with almost identical Al<sub>2</sub>O<sub>3</sub> and CaO concentrations, such as 15 and 27, 17 and 22, 2 and 14, 4 and 14, and 6 and 13, the Young's moduli always increase if SiO<sub>2</sub> is substituted by MgO.

Furthermore, glasses from Ref. [15] without any MgO were compared to similar glass compositions

from this glass series. In Table 3 and Fig. 3, the results are displayed and show a linear trend.

Marzouk et al. [40] stated that the formation of non-bridging oxygen reduces the network connectivity, weakens the glass structure and hence should result in decreasing Young's moduli. They are in agreement with El-Moneim and Alenezy [19], who suggested that due to an increase in the glass samples' rigidity, the elastic moduli should increase. On the contrary, DeGuire et al. [22] mentioned that it was long and wrongly believed that the weak ionic bonds between modifiers and non-bridging oxygens (meaning a lower network connectivity than for pure vitreous silica) are mainly responsible for decreasing Young's moduli: A higher silica concentration and

**Table 3** Shift of Young's modulus as function of difference of compositions Δ due to the substitution of SiO<sub>2</sub> by MgO in glasses

	SiO <sub>2</sub> (mol%)	CaO (mol%)	Al <sub>2</sub> O <sub>3</sub> (mol%)	MgO (mol%)	E modulus (GPa)
Glass 15	61.82	24.38	8.62	5.18	90.3
Glass 27	62.58	24.23	8.75	4.44	89.4
Δ	<b>-0.76</b>	<b>0.15</b>	<b>-0.13</b>	<b>0.74</b>	<b>0.9</b>
Glass 22	64.57	23.55	9.77	2.11	87.7
Glass 17	63.56	23.72	9.6	3.12	88.7
Δ	<b>1.01</b>	<b>-0.17</b>	<b>0.17</b>	<b>-1.01</b>	<b>-1</b>
Glass 14	63.02	24.66	9.23	3.09	87.6
Glass 2	62.58	24.75	9.27	3.41	88.9
Δ	<b>0.44</b>	<b>-0.09</b>	<b>-0.04</b>	<b>-0.32</b>	<b>-1.3</b>
Glass 4	61.6	24.51	9.23	4.67	88.3
Glass 14	63.02	24.66	9.23	3.09	87.6
Δ	<b>-1.42</b>	<b>-0.15</b>	<b>0</b>	<b>1.58</b>	<b>0.7</b>
Glass 17 [15]	66.385	23.863	9.752	0	84.4
Glass 21	62.522	23.798	9.723	3.957	88.2
Δ	<b>3.863</b>	<b>0.065</b>	<b>0.029</b>	<b>-3.957</b>	<b>-3.8</b>
Glass 17 [15]	66.385	23.863	9.752	0	84.4
Glass 17	63.564	23.718	9.599	3.119	88.7
Δ	<b>2.821</b>	<b>0.145</b>	<b>0.153</b>	<b>-3.119</b>	<b>-4.3</b>
Glass 15 [15]	64.856	26	9.145	0	85.3
Glass 23	60.913	25.887	9.189	4.011	88.9
Δ	<b>3.943</b>	<b>0.113</b>	<b>-0.044</b>	<b>-4.011</b>	<b>-3.6</b>
Glass 2 [15]	64.983	26.663	8.09	0.263	84.4
Glass 6	60.168	26.728	8.274	4.83	90.4
Δ	<b>4.815</b>	<b>-0.065</b>	<b>-0.184</b>	<b>-4.567</b>	<b>-6</b>
Glass 14 [15]	65.762	24.962	9.276	0	84.35
Glass 2	62.576	24.75	9.267	3.408	88.9
Δ	<b>3.186</b>	<b>0.212</b>	<b>0.009</b>	<b>-3.408</b>	<b>-4.55</b>

Variation of components are given in bold

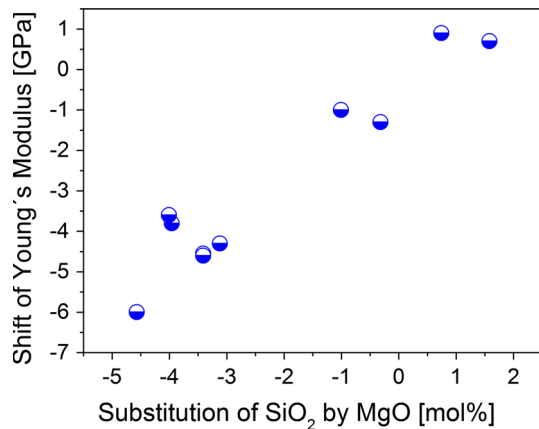


**Figure 3** Shift of Young's modulus as a function of difference of compositions  $\Delta$  due to substitution of SiO<sub>2</sub> by MgO.

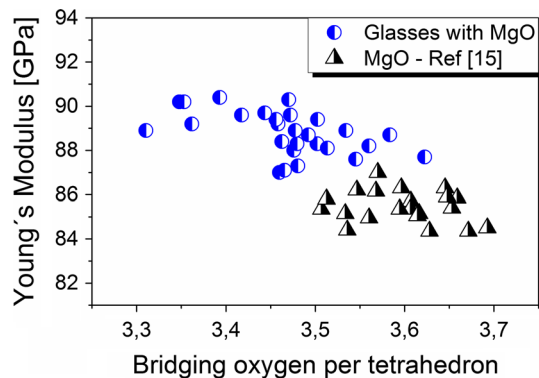


**Figure 4** Young's modulus as a function of the number of bridging oxygen per tetrahedron.

therefore a smaller network modifier concentration should lead to a higher network connectivity and hence a higher Young's modulus. However, they found just the opposite, increasing network connectivity results in decreasing Young's Modulus. The results in this paper confirm this observation. As shown in Fig. 4, the obvious trend shows an indirect proportionality: the higher the number of bridging oxygen—and hence the rigidity—of a glass sample, the lower the Young's modulus. Including the calcium oxide-aluminosilicate glasses from Ref. [15] which do not contain any MgO into the consideration, then a clear trend towards higher moduli with decreasing network connectivity (BOT/E) is observed. Incorporating a higher quantity of network modifiers such as CaO and MgO into the glass structure leads to a decrease in the quantity of bridging oxygens within the network. Hence, the glass with the highest concentration of the network

formers Al<sub>2</sub>O<sub>3</sub> and SiO<sub>2</sub> (glass 22) possesses the highest number of bridging oxygens per tetrahedron and therefore the highest network connectivity and also one of the lowest Young's modulus values with 87.7 GPa. The effect of decreasing Young's moduli with increasing SiO<sub>2</sub> concentrations within the glass system has also been reported in Ref. [15].

This can be explained by the fact that tightly packed glasses have higher elastic moduli than loosely packed glasses [18, 38]. A decrease in molar volume  $V_M$  (and hence an increase in packing density  $V_P$ ) will strengthen the resistance of the glass network to compression and hence increase the Young's modulus as shown in Fig. 5. The higher the network modifier concentration in the tested glasses is, the stronger is the decrease in the molar volume (see Fig. 5). This is due to the incorporation of the network modifiers into the network's cavities which triggers a contraction of the glass network, which has already been reported by Vogel [30] for alkali oxides. Also, a trend towards higher Young's moduli with increasing concentration of network modifiers and decreasing silica concentration is observed in Fig. 2.

Hence, Young's moduli of silicate glasses are mostly affected by the freedom of silicate tetrahedra to pivot about their connecting oxygens into the cavities of the network if network modifiers are incorporated. Hence, the packing density is increased and the freedom of movement of the oxygen ions is restricted. Thus, less strain may be accommodated by Si–O–Si bonds bending before adjacent ions touch or repel each other, which in turn increases the Young's modulus [18, 22, 38]. This connection between packing density  $V_P$  and Young's modulus was also visible for the studied glasses in Fig. 6.

This explains the Young's moduli decrease with increasing silica concentration, which is in contrast to the long-lasting opinion of increasing modulus with higher rigidity of the glass. Even though the correlation between SiO<sub>2</sub> concentration and the Young's modulus had been the most pronounced (with  $-0.57$ ), a high field strength of the network modifier has a larger effect on Young's moduli than the rigidity of the glass. So it can be concluded that competitive effects are influencing Young's modulus: The depolymerization results in lower network connectivity (and lower number of bridging oxygen per tetrahedron) which leads to decreasing Young's moduli, but this effect is (at least in this case) superimposed by the enhancement of Young's

**Figure 5** Young's modulus and packing density  $V_p$  as a function of the molar volume  $V_M$ .

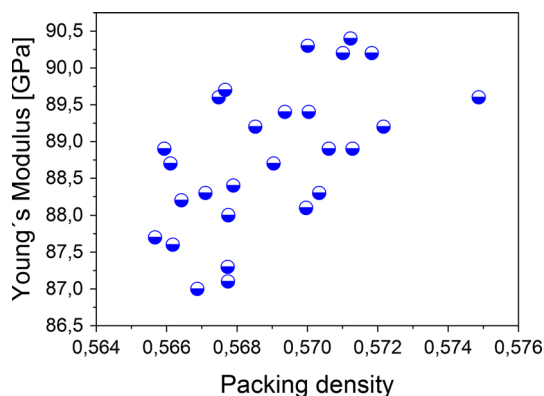
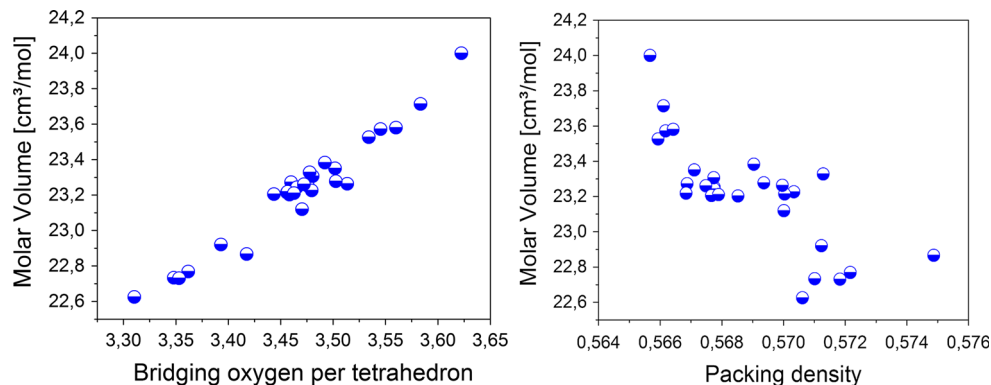


**Figure 6** Young's modulus as a function of the packing density  $V_p$ .

modulus due to the increasing cohesion with the addition of modifiers and hence the influence of this effect is larger.

In the case of the studied compositions, a good correlation was found between the elastic properties, the number of non-bridging oxygens, and in particular the packing density. This can, however, not be generalized. As stated by Rouxel [39], it is of importance also to include the energy density of volume into the discussion. He further reported that in most glasses an increasing energy density correlates well with an increasing bulk modulus; however, there are some discrepancies, which are depending mostly on the glass composition.

For the glass composition system which is discussed in this report, according to the energy density, different elastic properties would be predicted. For example, the elastic moduli of the investigated glass compositions increase with increasing aluminium concentration. This was found in alumina silicates as well; nevertheless, it is somewhat surprising to the author of Ref. [39], because the energy density is

decreasing due to fact that the Al–O bond (502 kJ/mol) is weaker than the Si–O bond (800 kJ/mol), and hence, the elastic moduli should also decrease. According to Ref. [39], this discrepancy can be explained by the different packing densities.

Moreover, if Ca is substituted by Mg, the elastic moduli decrease, which is also contradicting the calculation [41]: The bond strength of both cations is similar, the field strength of Mg is higher and hence the energy density is increasing, which means the elastic properties should increase as well. Again, this contradicting effect can be explained by the coordination of the ions and the packing density of the glass. The results of the glass systems from this paper do not show clear results for the observation made by Rouxel [39] and Deriano [41] regarding the exchange of Ca and Mg due to the small deviation of the values. However, it was found that CaO shows the larger effect on the elastic properties and is overshadowing the effects of MgO.

Furthermore, plots of the shear modulus and the bulk modulus against the Young's modulus are shown in Fig. 7. Both the shear and the bulk modulus have the same relations to the discussed parameters as the Young's modulus.

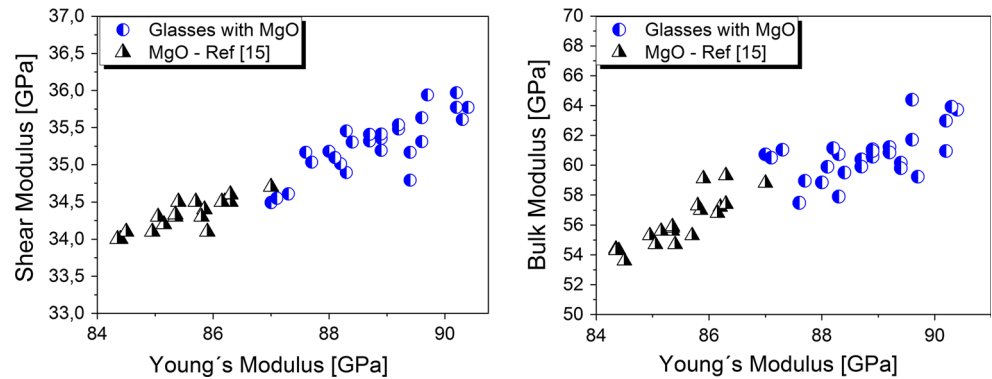
## Prediction of elastic properties

### Ultrasonic velocities

To predict the ultrasonic velocities of the characterized glasses, the methods developed by Priven [24], Demkina [42] and Makishima [17, 18] calculated via Sciglass version 6.6 [43] have been used.

The longitudinal phase velocities showed measured values varying between 6283 and 6438 m/s. The predicted values were between 5609 and 5651 m/s for Priven's estimation [24], 5418–5497 m/s for the method

**Figure 7** Bulk modulus and shear modulus as functions of Young's modulus.



by Makishima and Mackenzie [18] and between 5466 and 5582 m/s using Gan Fuxi's technique [44] for the longitudinal phase velocity in the glasses. In Fig. 8, the calculated values are plotted versus the measured results and the straight line in this figure is the line of 1:1 correlation (i.e. has a slope of unity). All three estimations are at least 600 m/s below the line of unity; the theoretical data are significantly lower than the measured ones. The calculated values by Priven [24] with a relatively small distribution of only 40 m/s are considerably smaller than the experimental data with a variation of 155 m/s. The Makishima calculation found values between 5418 and 5497 m/s, whereas Gan Fuxi's method [44] showed values in between these two simulations. Furthermore, the slope of the simulated data is not following the increasing trend of the measured data, demonstrating that all models are not suitable to simulate data within a small composition range.

The experimental data of the transversal phase velocity of the glasses varied between 3605 and 3673 m/s. The estimation described by Priven [24]

showed values from 3609 to 3649 m/s for the transversal velocities and the model by Gan Fuxi [44] from 3515 to 3586 m/s. Makishima & Mackenzie [43] is only simulating longitudinal velocity; therefore, no calculation by his method could be done. As shown in Fig. 8, the estimated data are closer to the experimental data set compared to the longitudinal phase velocity. The model by Priven [24] is also partly equal to the empirical values. Taking into account the machine error of  $\pm 30$  m/s, the values given by the calculations according to Priven are all within the error margin of the measurement and can be considered to be in agreement with the experimental data. Gan Fuxi's calculation [44] has a very high deviation, but the data are significantly out of the error margin of the experimental data, and the relative error is around 4%.

#### Poisson's ratio

To predict the Poisson's ratio, the method developed by Priven [24] calculated via Sciglass version 6.6 [43]

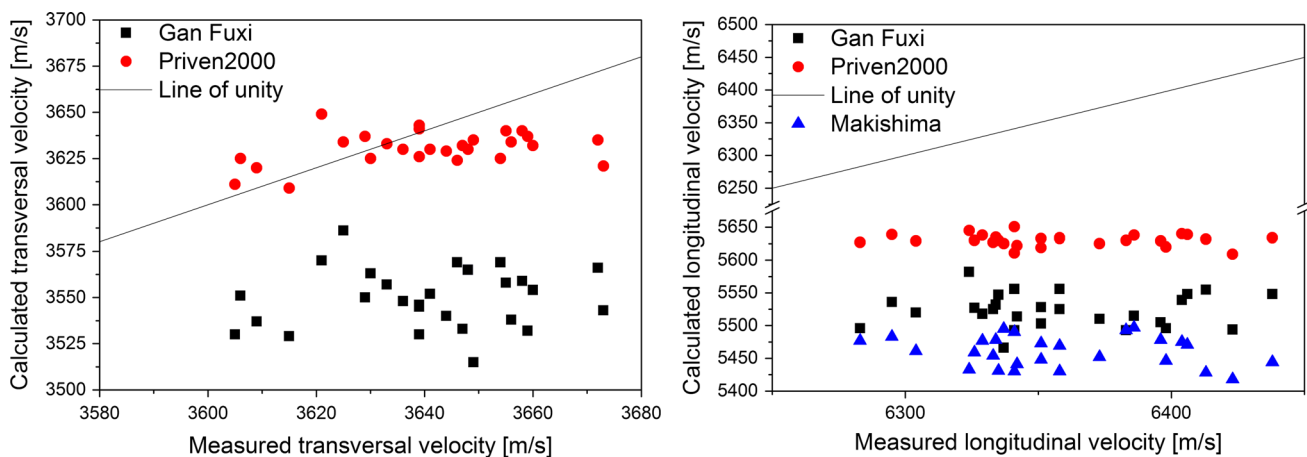


**Figure 8** Measured ultrasound velocities versus model calculations.

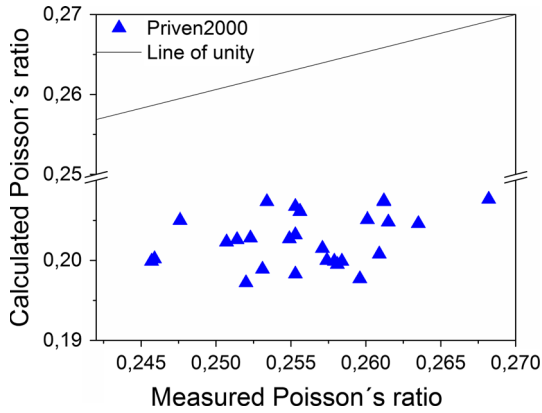
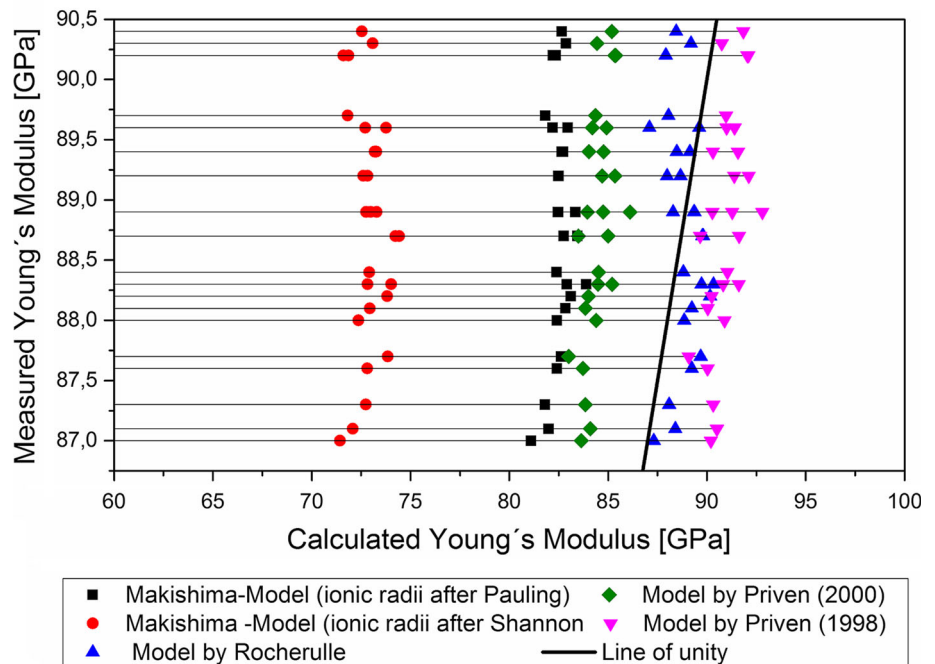


**Figure 9** Measured Poisson's ratio versus model calculations.

has been used. As shown in Fig. 9, the calculated values between 0.197 and 0.208 are around 0.06 below the measured data and hence show a very high relative error of 17 to 23%. Priven's calculation is not in agreement with the experimental values. It should be mentioned that Priven's results are also not in agreement with the theoretical values given by Rouxel, Bridge and Greaves [25, 38], who described that networks with a BO/T of 3 have Poisson's ratios of ~0.3 and networks with a BO/T of 4–0.15. If linearly extrapolated, the Poisson's ratio of a glass with a BO/T of 3.5 should be higher than 0.225.

**Figure 10** Measured Young's modulus versus model calculations.



*Young's modulus*

The experimental results of the elastic moduli were compared with predictions from existing empirical models. In Fig. 10, all computed values are displayed as a function of the measured values. The straight line in this figure is the line of 1:1 correlation (i.e. has a slope of unity).

One of the most widely used calculation models is that proposed by Makishima and Mackenzie in 1973 [17], which calculate Young's moduli  $E_{cal}$  of oxide glasses as function of the packing density  $V_p$  via the chemical compositions of the glasses and the dissociation energy of oxide constituents per unit volume according to the following equations:

$$E_{cal} = 83.6V_p \sum G_i x_i \tag{10}$$

where  $G_i$  is the dissociation energy (kcal) per unit volume ( $cm^3$ ). The  $G_i$  factor is obtained from the dissociation energy per unit volume

$$G_i = U_i \frac{\rho_i}{M_i} \tag{11}$$

where  $U_i$  is the dissociation energy (kcal) per mole of component  $i$ ,  $\rho_i$  is its density, and  $M_i$  is the molecular weight. The used values for  $U_i$ ,  $\rho_i$ ,  $M_i$  and  $G_i$  are displayed in Table 4. Lin and Liu [34] found in their

**Table 4** Density ( $\rho$ ), molar mass ( $M$ ), dissociation energy per mole of component  $i$  ( $U$ ), dissociation energy per unit volume ( $G$ ), packing factor calculated with Shannon's [46] and Pauling's [45] radii ( $V_i$ ), and the substitution factor for  $V_i$  by Rocherulle et al. [23] ( $C_i$ )

Oxide	SiO <sub>2</sub>	CaO	Al <sub>2</sub> O <sub>3</sub>	MgO
$\rho$ (g/cm <sup>3</sup> ) [47]	2.2	3.35	4.05	3.58
$M$ (g/mol)	60.08	56.0774	101.96	40.3044
$U$ (kcal/mol)/(kJ/mol) [48]	424/1775	257/1076	804/3366	222/930
$G$ (kcal/cm <sup>3</sup> )/(kJ/cm <sup>3</sup> )	15.5/64.9	15.4/64.5	31.9/133.6	19.7/82.5
$V_i$ (cm <sup>3</sup> /mol) with Pauling's radii	14.02	9.37	21.5	7.61
$V_i$ (cm <sup>3</sup> /mol) with Shannon's radii	12.46	8.73	18.92	7.15
$C_i$ [23]	0.6174	0.5530	0.8333	0.6750

work that using the density of quartz resulted in smaller deviations for low modulus glasses, whereas using the density of amorphous silica was better for the high modulus glasses. Therefore in this work, the density of amorphous silica was used as well. References [26, 38] reported that using the Makishima/Mackenzie model, it has been possible to calculate the Young's moduli for many silicate glasses with an accuracy of  $\sim 8\%$ , in particular for values  $<100$  GPa.

The values calculated by the Makishima/Mackenzie model for the glasses of this study are between 81.1 and 83.9 GPa and therefore around 6–7 GPa smaller than the measured ones. This is significantly out of the error margin of the experimental values.

It should be noted that for the calculation of the moduli, the atomic radii determined by Pauling [45] as described in Refs. [17, 18] and [23] were likewise used. But these radii do not take into account, in which coordination the ions occur. Especially for aluminium oxide, this is a problem concerning peraluminous or peralkaline melts. Although the empirical equations were designed for the use of Pauling's radii, it makes no sense to use ionic radii given by other authors. Nevertheless, if the atomic radii by Shannon [46] are used ( $0.39 \times 10^{-10}$ ,  $0.72 \times 10^{-10}$ ,  $1.00 \times 10^{-10}$ ,  $0.26 \times 10^{-10}$ , and  $1.35 \times 10^{-10}$  m for Al<sup>3+</sup>, Mg<sup>2+</sup>, Ca<sup>2+</sup>, Si<sup>4+</sup>, and O<sup>2-</sup>, respectively), the calculation of Young's moduli results in values between 70 and 73 GPa, which are hence at least ten GPa lower than the experimental values.

Rocherulle et al. [23] stated that the agreement of Makishima/Mackenzie model with measured calculations was good for a majority of their tested samples. However, they found that the correlation between the measured and calculated elastic modulus values is not satisfactory for values greater than 100 GPa. So some modifications were introduced for the packing factor of Makishima's model, in which

the factor  $G_i$  (see Eq. 7) was substituted by the calculated factors  $C_i$  (taken from Ref. [26]). The authors found a better agreement with their experimental values particularly for values greater than 80 GPa. Among Rocherulle et al.'s tested glasses was also a glass with 60 mol% SiO<sub>2</sub>, 30 mol% CaO and 10 mol% Al<sub>2</sub>O<sub>3</sub>, which is in the same composition range as the studied glasses. Its experimental Young's modulus was 86.2 GPa, and the calculated value according to Makishima was 80.8 GPa (both similar to our results). This is why Rocherulle et al.'s refinement of Makishima's calculation model was also applied to the glasses even though the Young's modulus of the glasses is only 87 GPa. The results are displayed in Fig. 10. These calculations gave values between 87 and 90 GPa. Values calculated using this method are closer to the experimental data and some even within the margin of error. The estimation by Rocherulle et al. gets better with increasing modulus, while the prediction of Makishima leads to increasing deviations to the real values and vice versa. Also in comparison with the glasses from Ref. [15] with slightly lower Young's moduli, the estimation is better.

Both calculations by the Rocherulle et al. and the Makishima/Mackenzie model use the experimentally determined density for the estimation, which means the prediction character is somewhat lost. If an empirically calculated value for the density is used, the propagation error increases immensely. In Ref. [27], a relative propagation error between 0.3 and 6% was found for the latest density models. A relative error of  $\pm 3\%$  of the estimated density values—which would lead to an absolute error of around 0.1 g/cm<sup>3</sup>—results in a deviation up to 4 GPa just for the glass compositions of this paper. It might be even higher for other compositions with more or different components. Thus, the error of the models for density cannot be fully eliminated by the model calculations; the final error of both estimation methods will be

even higher. Therefore, this cannot be considered as an advantageous model calculation because the real error also depends on the unknown error of the density calculation.

Additionally, the Young's moduli have been calculated by the two methods proposed by Priven [24] using Sciglass 6.6 [43]. The calculations by Priven's method [24] are based on semi-empirical formulas similar to the chemical equilibria equations.

The values 83.0 to 86.1 GPa calculated via the method "Priven 2000" are lower than the data range of the older version "Priven 1998," which are between 89.1 and 92.8 GPa. They are both higher than the values calculated using the method of Makishima. "Priven 1998" data are even exceeding Rocherulle and his group's calculation and the line of unity, whereas the method "Priven 2000" is underestimating the Young's moduli of the glasses.

All calculation methods show the same deviation of around 3 GPa from the measured values, which is equal to the distribution of the actual determinations even though the actual values show shifts from 71 to 93 GPa.

Even though the approximation of Rocherulle et al. is closest to the experimental values, the model "Priven 2000" is considered as the best fitting one in this case. This is due to the fact that Rocherulle et al.'s estimation was calculated with real density results in this case and would be farther off if approximated density data were used.

## Conclusions

The measured Young's moduli were between 87 and  $90.5 \pm 0.8$  GPa. The comparatively small variations of composition had only a small effect on the tested properties, although significantly larger than the estimated propagation error. The Young's modulus decreases with increasing mean number of bridging oxygens per tetrahedron. Young's modulus was most strongly affected by the concentration of network modifiers: the higher the concentration of network modifiers, the higher the Young's modulus even though the depolymerization is also increasing and hence the network rigidity is decreasing. The increasing packing density if network modifiers are added to the compositions leads to a higher resistance of deformation and hence an increase in the

Young's moduli even though the network structure is depolymerized.

The ultrasonic phase velocities show no clear correlation with the number of bridging oxygens within the glasses, although the Poisson's ratio, which was derived from the phase velocities, correlates with an indirect proportionality. It increases with the number of bridging oxygens, which is explained by the increasing network rigidity. Nearly all model predictions for the phase velocities of the glasses by different authors are not in agreement with the measured results for the phase velocities.

The Makishima/Mackenzie model for the calculation of Young's Moduli gives acceptable results if Pauling's atomic radii for the ions are used [45]. Using Shannon's ionic radii [46] and taking the coordination of the ions into account, the agreement with the experimental data is worse. Rocherulle et al.'s enhancement of the Makishima/Mackenzie theory yields higher values than the measurement; however, they are closer to the measured data. Nevertheless, the results for both Makishima/McKenzie and Rocherulle et al.'s models are only close because experimental density values were used for the calculations. If the density would also be predicted by some model, the deviation of values would increase 6 GPa if the model has a relative error of 5%. The models by Priven [24] are closest in comparison with the other models. Due to the fact that no value for the density is needed for the calculation with Priven's Methods, they are considered to be the best for a rough estimation of Young's modulus.

## Acknowledgements

This study was funded by 3B-The Fibreglass Company. S and T Center. Rue de Charneux, 59. 4651 Battice, and the Walloon Region, Belgium. The authors thank Yves Houet and Dimitri Laurent for the measurement of the X-ray fluorescence data and helpful technical counsel.

## References

- [1] Dittmer M, Rüssel C (2012) Colorless and high strength MgO/Al<sub>2</sub>O<sub>3</sub>/SiO<sub>2</sub>-glass-ceramic dental material using zirconia as nucleating agent. *J Biomed Mater Res B* 100:463–470

- [2] Berndt S, Gawronski A, Patzig C et al (2015) Oriented crystallization of a beta-Quartz Solid Solution from a MgO/Al<sub>2</sub>O<sub>3</sub>/SiO<sub>2</sub> glass in contact with tetragonal ZrO<sub>2</sub> ceramics. *RSC Adv* 5(20):15164–15171
- [3] Dittmer M, Yamamoto CF, Bocker C, Rüssel C (2011) Crystallization and mechanical properties of MgO/Al<sub>2</sub>O<sub>3</sub>/SiO<sub>2</sub>/ZrO<sub>2</sub> glass–ceramics with and without the addition of yttria. *Solid State Sci* 13:2146–2153
- [4] Wallenberger FT (2010) *Fiberglass and Glass technology: energy friendly compositions and applications*. Springer, New York
- [5] Wallenberger FT, Smrcek A (2010) The liquidus temperature; its critical role in glass manufacturing. *Int J Appl Glass Sci* 1(2):151–163
- [6] Veit U, Houet Y, Laurent D, Rüssel C (2015) Liquidus temperatures of calcium magnesium aluminosilicate glass-forming compositions determined via gradient furnace and from the melting peak by differential thermal analysis. *Thermochim Acta* 618:1–5
- [7] Tiegel M, Herrmann A, Rüssel C et al (2013) Magnesium aluminosilicate glasses as potential laser host material for ultrahigh power laser systems. *J Mater Chem C* 1:5031–5039. doi:10.1039/C3TC30761A
- [8] Tiegel M, Hosseiniabadi R, Kuhn S, Herrmann A, Rüssel C (2015) Young's modulus, Vickers hardness and indentation fracture toughness of alumino silicate glasses. *Ceram Int* 41(6):7267–7275
- [9] Herrmann A, Rüssel C (2015) New aluminosilicate glasses as high-power laser materials. *Int J Appl Glass Sci* 6(3):210–219. doi:10.1111/ijag.12127
- [10] Shin JW, Wilsmann W, Conradt R (2005) Thermochemical and physical properties of glasses based on the system CaO–MgO–Al<sub>2</sub>O<sub>3</sub>–SiO<sub>2</sub>. *Phys Chem Glasses* 46:128–131
- [11] Song M, Shu Q, Sichen D (2011) Viscosities of the quaternary Al<sub>2</sub>O<sub>3</sub>–CaO–MgO–SiO<sub>2</sub>-slags. *Steel Res Int* 82:260–268
- [12] Kraxner J, Klement R, Chromčíková M et al (2008) The effect of CaO and MgO on physical properties of MgO–CaO–B<sub>2</sub>O<sub>3</sub>–Al<sub>2</sub>O<sub>3</sub>–SiO<sub>2</sub> glasses with composition close to the E-glass fibers. *Adv Mater Res* 39–40:81–84
- [13] Abel BM, Mauro JC, Smedskjaer MM et al (2013) Liquidus surface of MgO–CaO–Al<sub>2</sub>O<sub>3</sub>–SiO<sub>2</sub> glass-forming systems. *J. Non-Cryst Solid* 363:39–45
- [14] Koch K, Trömel G, Heinz G (1975) "Das Zustandsdiagramm Al<sub>2</sub>O<sub>3</sub>–CaO–MgO–SiO<sub>2</sub> in polythermischer Darstellung, Tonind.-Ztg. *Keram. Rundsch* 99(3):57–62
- [15] Veit U, Rüssel C (2016) Density and young's modulus of ternary glasses close to the eutectic composition in the CaO–Al<sub>2</sub>O<sub>3</sub>–SiO<sub>2</sub>-system. *Ceram Int* 42:5810–5822. doi:10.1016/j.ceramint.2015.12.123
- [16] Hwa L-G, Hsieh K-J, Liu L-C (2003) Elastic moduli of low-silica calcium alumino-silicate glasses. *Mater Chem Phys* 78(1):105–110
- [17] Makishima A, Mackenzie JD (1973) Direct calculation of Young's modulus of glass. *J Non-Cryst Solids* 12:35–45
- [18] Makishima A, Mackenzie JD (1975) Calculation of bulk modulus, shear modulus and Poisson's ratio of glass. *J Non-Cryst Solids* 17:147–157
- [19] El-Moneim AA, Alenezy A (2013) Structural and acoustic properties of lead silicate glasses doped with alkali and alkaline earth oxides. *Phys Chem Glasses Eur J Glass Sci Technol B* 54(5):232–237
- [20] Saddeek YB, Latif LAE (2004) Effect of TeO<sub>2</sub> on the elastic moduli of sodium borate glasses. *Phys B* 348:475–484
- [21] Hwa L-G, Lua C-L, Liu L-C (2000) Elastic moduli of calcium alumino-silicate glasses studied by Brillouin scattering. *Mater Res Bull* 35:1285–1292
- [22] DeGuire M, Brown SD (1984) Dependence of Young's modulus on volume and structure in alkali silicate and alkali aluminosilicate glasses. *J Am Ceram Soc* 67:270–273. doi:10.1111/j.1151-2916.1984.tb18845.x
- [23] Rocherulle J, Ecolivet C, Poulain M et al (1989) Elastic moduli of oxynitride glasses. *J Non-Cryst Solids* 108:187–193
- [24] Priven AI (2004) General method for calculating the properties of oxide glasses and glass forming melts from their composition and temperature. *Glass Technol* 45:244–254
- [25] Bridge B, Patel ND, Waters DN (1983) On the elastic constants and structure of the pure inorganic oxide glasses. *Phys Stat Sol (a)* 77:655
- [26] Inaba S, Fujino S, Morinaga K (1999) Young's modulus and compositional parameters of oxide glasses. *J Am Ceram Soc* 82(12):3501–3507
- [27] Veit U, Rüssel C (2014) Density of quaternary glasses in the MgO–CaO–Al<sub>2</sub>O<sub>3</sub>–SiO<sub>2</sub>-system: modeling versus measurement. *Int J Appl Glass Sci*. doi:10.1111/ijag.12263
- [28] PhD-Thesis (2014) Antje Gawronski, Jena University
- [29] Walter G, Vogel J, Hoppe U, Hartmann P (2003) Structural study of magnesium polyphosphate glasses. *J Non-Cryst Solids* 320(1-3):210–222
- [30] Vogel W (1994) *Glass chemistry*, 2nd edn. Springer, Berlin
- [31] ASTM C693-93 (2013) Standard test method for density of glass by buoyancy, ASTM international, West Conshohocken, PA. doi:10.1520/C0693, [www.astm.org](http://www.astm.org)
- [32] Krautkrämer J, Krautkrämer H (1969) *Ultrasonic testing of materials*. Springer, Berlin
- [33] Hill R (1963) Elastic properties of reinforces solids: some theoretical principles. *J Mech Phys Solids* 11(5):357–372
- [34] Lin C-C, Liu L-G (2006) Composition dependence of elasticity in aluminosilicate glasses. *Phys Chem Miner* 33:332–346



- [35] Shelby JE (2005) Introduction to glass science and technology, 2nd edn. The Royal Society of Chemistry, Cambridge
- [36] Löwenstein W (1954) The distribution of aluminum in the tetrahedra of silicates and aluminates. *Am Miner* 39:92–96
- [37] Gaafar MS, Marzouk SY (2007) Mechanical and structural studies on sodium borosilicate glasses doped with  $\text{Er}_2\text{O}_3$  using ultrasonic velocity and FTIR spectroscopy. *Phys B* 338:294–302
- [38] Greaves GN, Greer AL, Lakes RS, Rouxel T (2011) Poisson's ratio and modern materials. *Nat Mater* 10:823–836
- [39] Rouxel T (2007) Elastic properties and short-to medium-range order in glasses. *J Am Ceram Soc* 90:3019–3039
- [40] Marzouk SY (2010) The acoustic properties of borosilicate glass affected by oxide of rare earth gadolinium. *Phys B* 405:3395–3400
- [41] Deriano S, Rouxel T, Lefloch M, Beuneu B (2004) Structure and mechanical properties of alkali-alkaline earth-silicate glasses. *Phys Chem Glass* 45:37–44
- [42] Volf MB (1988) Mathematical approach to glass-glass science and technology 9. Elsevier, Amsterdam
- [43] Sciglass (2006) MDL<sup>®</sup> SciGlass, version 6.6. MDL Information Systems, Inc., San Leandro
- [44] Gan Fuxi (1963) New system of calculation of some physical properties of silicate glasses. *Sci Sinica* 12(9):1365–1391
- [45] Pauling L (1960) Nature of chemical bond and structure of molecules and crystals, 3rd edn. Cornell University Press, Ithaca
- [46] Shannon RD (1976) Revised effective ionic radii and systematic studies of interatomic distances in halides and chalcogenides. *Acta Cryst A* 32:751–767
- [47] Lide DR (ed) (2008) CRC handbook of chemistry and physics, 89th edn. CRC Press, Boca Raton
- [48] Huggins ML, Sun K-H (1943) Calculation of density and optical constants of a glass from its composition in weight percentage. *J Am Ceram Soc* 30(1):4–11